

Comparison of quantum cascade structures for detection of nitric oxide at $\sim 5.2 \mu\text{m}$

Andrzej Kolek

Department of Electronics Fundamentals
Rzeszow University of Technology
Rzeszów, Poland

Grzegorz Hałdaś

Department of Electronics Fundamentals
Rzeszow University of Technology
Rzeszów, Poland

Maciej Bugajski

Institute of Electron Technology
Warsaw, Poland

Abstract—Nonequilibrium Green’s function method is used to calculate electronic and optical characteristics of various quantum cascade structures emitting light at $\sim 5.2 \mu\text{m}$ wavelength. Basing on these simulations, the choice of optimal design can be done.

Index Terms—nonequilibrium Green’s function, quantum cascade laser, electronic transport, optical gain, electron-photon selfenergy

I. INTRODUCTION

The design of quantum structures utilized in modern optoelectronic devices is crucial for their performance. The latter, obviously, depends on the evaluation criteria; however, even if these criteria are well established, the choice of optimally designed structure is not easy because devices that use nominally the same structure very often exhibit quite different experimental characteristics. Mostly, this is due to device processing-dependent factors, like leakage or serial resistance, which still contribute much to the final device characteristics and influence them in unpredictable manner. Due to this limitation, the evaluation of quantum structures in terms of their ability to effectively absorb or gain the light basing exclusively on experimental data appears as a big challenge. For these purposes, numerical simulations seem to be helpful, because they are able to provide data that can be exclusively related to the design of quantum structures responsible for light generation/absorption, and so can be used for their evaluation. The condition that must be fulfilled to assure this conjecture is that proper simulation method is used and quantum structure is modeled with sufficient accuracy. One of them is nonequilibrium Green’s function (NEGF) formalism [1, 2] which is used in this paper to compare quantum cascade structures emitting light at $\sim 5.2 \mu\text{m}$ wavelength. These structures receive much interest due to their use in NO detection systems [3] important in numerous applications. The use of NEGF method to achieve a valuable result is almost a must because in this method coherent phenomena, like quantum tunneling, are simultaneously included with the scattering processes that break phase coherence.

This research was supported by the National Centre for Research and Development grant no. TECHMATSTRATEG1/347510/15/NCBR/2018 (SENSE).

II. MODEL AND METHOD

QCLs are unipolar, n-type devices, so the single-band effective mass Hamiltonian provides a sufficient description. In this Hamiltonian, the influence of valence band was included assuming the effective mass of the particle depends on its total energy E . The linear form $m(E) = m^*[1 + (E - E_c)/E_g]$ was assumed for this dependence with the values of the parameters: m^* and E_g evaluated from tight binding sp³d⁵s* model of the band structure of the constituents building the QCL device, like in [4]. Conduction bandgap offsets between these constituents were calculated basing on model-solid theory including strain [5] and material parameters taken from [6]. This method was also used to evaluate bandgap offsets (0.42 eV for InGaAs and 1.53 eV for InAlAs) used in the parametrization of alloy disorder scattering.

The stratified structure of QCLs allows to simplify the device Hamiltonian to 1D equation in the growth (z) direction with in-plane kinetic energy term $\hbar^2 k^2 / 2m(E, z)$, where $k = |\mathbf{k}|$ is the magnitude of the in-plane momentum \mathbf{k} .

The calculations were made in the position basis: the base vectors were defined by the points discretizing the device Hamiltonian at certain z -axis positions. As QCL core is periodic, the structure subjected to the calculations was limited to a bit more than one QCL period connected to the leads that reliably imitated device periodicity [7]. The scatterings occurring in the device were included in the form of appropriate selfenergies incorporated into NEGF equations. The formulations for contact and scattering selfenergies were taken from [1] for LO-phonon, interface roughness, ionized impurity and alloy disorder scatterings, whereas for the acoustic phonons the approximation of [2] was used. For electron-photon interaction, the selfenergies were calculated as in [8]. The equations of NEGF formalism were solved for the steady state. Then, the gain/absorption was calculated basing on the theory outlined in [9], adopted for the case of energy-dependent effective mass [10].

III. RESULTS

Calculations were made for 4 quantum cascade structures used in the devices that emit radiation at $\sim 5.2 \mu\text{m}$ wavelength. Details of these structures can be found respectively in [11] for structure E, in [12] for structure D, in [13] for structure C, and in [14] for structure K. The comparison was done at

near room temperature of 288 K. It was also assumed that the devices have the same number of periods (30) and were doped to the same sheet density ($n_{\text{dop}} = 0.89 \times 10^{11} \text{ cm}^{-2}$ per period), although different doping profiles proposed by their designers were maintained. Identical interface roughness height $\Delta = 0.19 \text{ nm}$ and correlation length $\Lambda = 9 \text{ nm}$ were assumed for all devices. The evaluation criteria were adopted from end-users practice, namely: the parameters like maximum gain, maximum output power or minimum current threshold were compared. For these purposes, the simulations were done for light-matter interaction either included or excluded from the calculations. For the former, the photon flux was increased until the gain was clamped to its threshold value, $g_{\text{th}} = 9.5 \text{ cm}^{-1}$, corresponding to the overall losses in a typical waveguide. Then, the light power was estimated for one facet of $10 \mu\text{m}$ -wide cavity. The results of the simulations are presented in Figs. 1 and 2. In Fig. 1, the current-voltage and gain-current characteristics are shown for the case without light-matter interaction included in the calculations. The performance parameters read-out from these characteristics are gathered in Table I: the maximum gain of $\sim 30 \text{ cm}^{-1}$ is observed for the structures E and D, whereas the minimum threshold current has the structure K. Maximum optical power can be achieved in the structure E. This value was estimated from light-current characteristics calculated with electron-photon selfenergies included in the calculations. Such simulations were performed only for the structures E and D which exhibit the largest gain peak. As can be seen in Fig. 2, the optical power available from these structures can differ significantly, even though they have almost equal peak values of the gain.

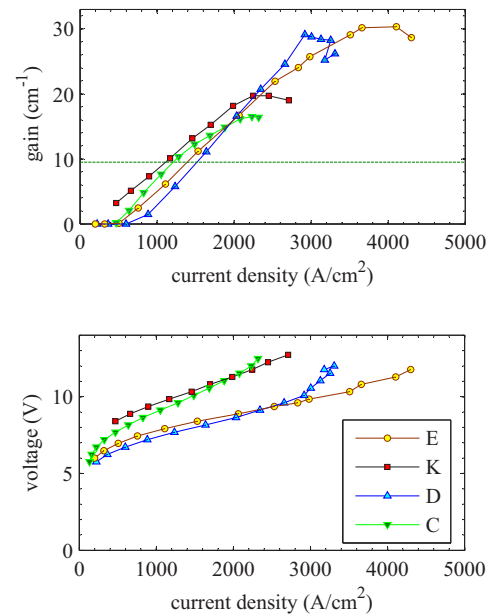


Figure 1. Current-voltage (upper) and gain-current (lower) characteristics calculated for the structures E, D, C, and K with the NEGF method without electron-photon selfenergies. Horizontal line in lower figure is drawn at the threshold value g_{th} .

Table I
PERFORMANCE PARAMETERS OF DIFFERENT QCL STRUCTURES

Structure	Threshold current	Gain peak	Light power
E	1400 Acm^{-2}	30 cm^{-1}	0.94 W
D	1550 Acm^{-2}	29 cm^{-1}	0.61 W
C	1220 Acm^{-2}	16 cm^{-1}	x
K	1100 Acm^{-2}	20 cm^{-1}	x

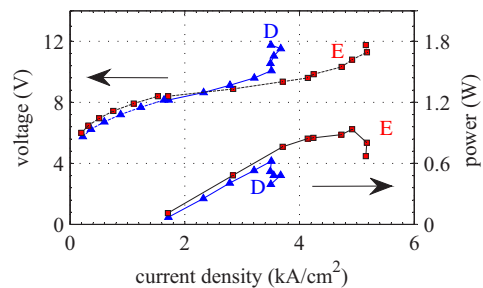


Figure 2. Current-voltage and light-current characteristics calculated for the structures E and D with the NEGF method including electron-photon selfenergies.

REFERENCES

[1] R. Lake, G. Klimeck, R. C. Bowen, and D. Jovanovic, *J. Appl. Phys.*, vol. 81 (12), p. 7845–7869, February 1997.

[2] T. Kubis *et al.*, *Phys. Rev. B.*, vol. 79 (19), p. 195323, May 2009.

[3] P. Kluczynski, S. Lundqvist, J. Westberg, and O. Axner, *Appl. Phys. B*, vol. 103 (2), pp. 451–459, May 2011.

[4] T. Kato and S. Souma, *J. Appl. Phys.*, vol. 125 (7), p. 073101, February 2019.

[5] Ch. G. Van de Walle, *Phys. Rev. B*, vol. 39 (3), pp. 1871–1883, January 1989.

[6] I. Vurgaftman, J. R. Meyer, and L. R. Ram-Mohan, *J. Appl. Phys.*, vol. 89 (11), pp. 5815–5875, June 2001.

[7] G. Hałdaś, A. Kolek, and I. Tralle, *IEEE J. Quantum Electron.*, vol. 47 (6), pp. 878–885, May 2011.

[8] A. Kolek, in 2018 International Conference on Numerical Simulation of Optoelectronic Devices (NUSOD), J. Piprek and A. B. Djurišić, Eds., pp. 51–52, November 2018.

[9] S.-C. Lee and A. Wacker, *Phys. Rev. B*, vol. 66 (24), p. 245314, December 2002.

[10] A. Kolek, *Appl. Phys. Lett.*, vol. 106 (18), p. 181102, May 2015.

[11] A. Evans *et al.*, *Appl. Phys. Lett.*, vol. 88 (5), p. 051105, January 2006.

[12] L. Diehl *et al.*, *Appl. Phys. Lett.*, vol. 89 (8), p. 081101, August 2006.

[13] R. A. Cendejas *et al.*, *IEEE Photonics J.*, vol. 3 (1), pp. 71–81, January 2011.

[14] F. Kapsalidis *et al.*, *Appl. Phys. B*, vol. 124 (6), p. 124107, May 2018.